

## MOCVD OF PEROVSKITES WITH METALLIC CONDUCTIVITY

O.YU. GORBENKO, A.R. KAUL, A.A. MOLODYK, M.A. NOVOZHILOV,  
A.A. BOSAK

Chemistry Department, Moscow State University, 119899 Moscow, Russia

N.A. BABUSHKINA, L.M. BELOVA

Kurchatov Institute, 123182 Moscow, Russia

U. KRAUSE AND G. WAHL

IOPW, TU Braunschweig, Bienroder Weg 53, 38108 Braunschweig, Germany

Single source MOCVD techniques were used to prepare perovskite films with metallic conductivity ( $\text{CaRuO}_3$ ,  $\text{LaNiO}_3$ ,  $\text{La}_{0.5}\text{Sr}_{0.5}\text{CoO}_3$  and  $(\text{La, Pr})_{0.7}(\text{Sr, Ca})_{0.3}\text{MnO}_3$ ). Structural and electrical properties of the epitaxial layers on the coherent substrates are close to that of the films grown by pulsed laser deposition and magnetron sputtering. Peculiarities of the growth occur on the worse matched substrates, such as a mixture of two orientations, each aligned in the plane of the interface ( $\text{LaNiO}_3/\text{MgO}$ ) and variant structures in the films on yttrium stabilized zirconia. X-ray diffraction of the films indicates pseudocubic lattice for all  $\text{R}_{1-x}\text{A}_x\text{MO}_3$  films in spite of the distortions in the bulk material. The dependence of metal-insulator transition in  $\text{R}_{1-x}\text{A}_x\text{MnO}_3$  on the nature of R and A and film-substrate lattice mismatch was studied.

PACS numbers: 81.15.Gh, 68.55.-a

Thin films of  $\text{R}_{1-x}\text{A}_x\text{MO}_3$  perovskites with metallic conductivity, where R is rare-earth element, A — alkaline-earth element and M — transition metal, have attracted much attention for various applications such as fatigue resistant electrodes for ferroelectric layers [1], metal layers in superconductor/normal metal/superconductor (SNS) junctions [2], high temperature refractory electrodes [3], gas sensors [4] and oxidation catalysts [5]. On the other hand, the nature of the metallic state in perovskites as well as their relation to the superconducting cuprates were subject of numerous studies [6]. Metal-insulator transition (M-I) was observed in the various  $\text{R}_{1-x}\text{A}_x\text{MO}_3$  compounds [7]. The discovery of giant magnetoresistance (GMR) effects in  $\text{R}_{1-x}\text{A}_x\text{MnO}_{3+y}$  has attracted even more interest to the materials [8].

TABLE I

Parameters of the deposition processes.

Parameter	Band flash evaporation	Powder flash evaporation	Aerosol MOCVD
Stagnation flow reactor type	cold wall	hot wall	cold wall
Deposition temperature [°C]	750–850	800–850	750
Total pressure [mbar]	13	13	6
Total gas flow [l/h]	60	20	20
Partial pressure of O <sub>2</sub> [mbar]	1.45	6	3
Deposition rate [μm/h]	0.2–0.7	0.2–0.5	0.5–1
Solvent* consumption [ml/h]	no	no	20
Evaporator temperature [°C]	250	250	250

\*diglyme (CH<sub>3</sub>OCH<sub>2</sub>CH<sub>2</sub>OCH<sub>2</sub>CH<sub>2</sub>OCH<sub>3</sub>) with 5 vol.% Ithd.

In the current work we have prepared R<sub>1-x</sub>A<sub>x</sub>MO<sub>3</sub> films by the perspective single source metal-organic chemical vapour deposition (MOCVD) and studied their structure and electrical properties.

Three versions of single source MOCVD described in detail elsewhere were used, namely, flash powder evaporation [9], band flash evaporation [10] and aerosol MOCVD [11]. The deposition conditions are summarized in Table I. The R<sub>1-x</sub>A<sub>x</sub>MO<sub>3</sub> prepared were LaNiO<sub>3</sub>, CaRuO<sub>3</sub>, La<sub>1-x</sub>Sr<sub>x</sub>CoO<sub>3</sub> ( $x = 0-0.5$ ), (La<sub>1-x</sub>Pr<sub>x</sub>)<sub>0.7</sub>(Sr, Ca)<sub>0.3</sub>MnO<sub>3</sub> ( $x = 0-1$ ), single crystal substrates — LaAlO<sub>3</sub>, SrTiO<sub>3</sub>, MgO, yttria stabilized zirconia (YSZ), buffer layers — PrO<sub>x</sub>/YSZ, CeO<sub>2</sub>/YSZ, CeO<sub>2</sub>/Al<sub>2</sub>O<sub>3</sub>. Volatile precursors were as follows: La(thd)<sub>3</sub>, Pr(thd)<sub>3</sub>, Sr(thd)<sub>2</sub>, Ca(thd)<sub>2</sub>, Co(thd)<sub>2</sub>, Ru(acac)<sub>3</sub>, Mn(thd)<sub>3</sub>, Ni(thd)<sub>2</sub> and Ni(acim)<sub>2</sub>, where acac is acetylacetonate, thd — 2,2,6,6-tetramethylheptan-3,5-dionate, acim — acetylacetoniminate. X-ray diffraction (XRD) with four-circle diffractometer Siemens D5000 was applied to determine phase composition, orientation and lattice parameters. Scanning electron microscopy (SEM) was accomplished by CAMSCAN equipped with EDAX system for quantitative analysis. Electrical resistance  $R(T)$  was measured by the standard ac four-probe technique with silver contacts in the range 77–300 K.

XRD patterns of R<sub>1-x</sub>A<sub>x</sub>MO<sub>3</sub> films (Fig. 1) look like that of cubic lattice without any splitting of (00 $l$ ) or ( $h$ h0) reflexes or superstructural peaks. It does not mean that the perovskite film is necessarily cubic because of the film orientation.  $\theta-2\theta$  scan reveals preferable orientation (001)<sub>f</sub> || (001)<sub>s</sub>, where indices f and s mean film and substrate (LaAlO<sub>3</sub>, SrTiO<sub>3</sub>, MgO), respectively. Perovskite substrates (LaAlO<sub>3</sub>, SrTiO<sub>3</sub>) permit deposition of the layers showing only (00 $l$ ) reflexes,  $\varphi$ -scans prove the epitaxy of the "cube-on-cube" type. Rocking curves for (00 $l$ ) reflexes have FWHM 0.17–0.25 deg, which indicates the high epitaxial quality of the films. La<sub>1-x</sub>Sr<sub>x</sub>CoO<sub>3</sub> was grown on MgO with the pure (001) orientation up to 2500 Å thick. XRD patterns of R<sub>1-x</sub>A<sub>x</sub>MnO<sub>3</sub>/MgO reveal (110) peak

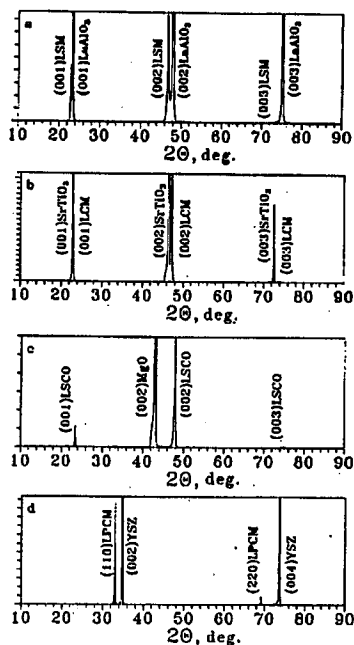


Fig. 1. Typical  $\theta$ - $2\theta$  scans :  $\text{La}_{0.7}\text{Sr}_{0.3}\text{MnO}_3/\text{LaAlO}_3$  (a),  $\text{La}_{0.7}\text{Ca}_{0.3}\text{MnO}_3/\text{SrTiO}_3$  (b),  $\text{La}_{0.5}\text{Sr}_{0.5}\text{CoO}_3/\text{MgO}$  (c),  $\text{La}_{0.35}\text{Pr}_{0.35}\text{Ca}_{0.3}\text{MnO}_3/\text{YSZ}$  (d).

at the thickness  $> 2000 \text{ \AA}$ .  $\text{LaNiO}_3$  demonstrates  $(00l)$  and  $(hh0)$  reflexes always, with  $(001)$  and  $(110)$  reflexes of the comparable intensity for the film  $> 500 \text{ \AA}$  thick. Large lattice mismatch between  $\text{MgO}$  ( $a = 4.21 \text{ \AA}$ ) and  $\text{R}_{1-x}\text{A}_x\text{MO}_3$  ( $a = 3.80\text{--}3.90 \text{ \AA}$ ) hinders the epitaxy of the film. The appearance of the admixture texture does not correlate directly with the lattice mismatch, which is greater for  $\text{La}_{1-x}\text{Sr}_x\text{CoO}_3$  than for  $\text{LaNiO}_3$ .

According to  $\varphi$ -scans  $(001)$  oriented domains on  $\text{MgO}$  have good in-plane alignment: fourfold degeneracy of peaks is observed at the tilt angle equal to that between the plane under study and  $(001)$  plane. Rocking curves for  $(00l)$  planes with  $\text{FWHM} \approx 0.5^\circ$  were measured for best  $\text{La}_{1-x}\text{Sr}_x\text{CoO}_3$  and  $\text{R}_{1-x}\text{A}_x\text{MnO}_3$ . For  $\text{LaNiO}_3$  fourfold symmetry was observed at the tilt angles referred to both  $(001)_{\text{LaNiO}_3} \parallel (001)_{\text{MgO}}$  and  $(110)_{\text{LaNiO}_3} \parallel (001)_{\text{MgO}}$ . Hence, both orientations are aligned in the plane.  $\text{FWHM}$  of  $(00l)$  and  $(hh0)$  rocking curves are  $0.8\text{--}1^\circ$  and  $1.2\text{--}2^\circ$  respectively.

$\text{R}_{1-x}\text{A}_x\text{MO}_3$  perovskites on  $\text{YSZ}$  have preferable orientation  $(110)_f \parallel (001)_{\text{YSZ}}$ .  $\varphi$ -scans reveal 4-component variant structure, caused by the diagonal epitaxy with  $[1\text{--}11]_f \parallel [110]_{\text{YSZ}}$  and  $[1\text{--}11]_f \parallel [1\text{--}10]_{\text{YSZ}}$ . Pure  $(110)_f \parallel (001)_{\text{YSZ}}$  orientation can be obtained for manganites, but  $\text{CaRuO}_3$  and

$\text{La}_{1-x}\text{Sr}_x\text{CoO}_3$  films contain an admixture texture  $(001)_f \parallel (001)_{\text{YSZ}}$ . The result correlates to the diagonal match with YSZ ( $a\sqrt{3}$  to  $5.14\sqrt{2}$ ). The FWHM of the rocking curves of the reflex (220) shows similar behaviour:  $> 1^\circ$  for  $\text{La}_{1-x}\text{Sr}_x\text{CoO}_3$ ,  $0.77^\circ$  for  $\text{CaRuO}_3$ ,  $0.58^\circ$  for  $\text{La}_{0.7}\text{Sr}_{0.3}\text{MnO}_3$ .  $\text{CeO}_2$  and  $\text{PrO}_x$  buffer layers on YSZ switch the film orientation to  $(001)_f \parallel (001)_{\text{CeO}_2} \parallel (001)_{\text{YSZ}}$ .

$\text{La}_{0.5}\text{Sr}_{0.5}\text{CoO}_3$  and  $\text{La}_{0.7}\text{Sr}_{0.3}\text{MnO}_3$  films on  $\text{SiO}_2/(111)\text{Si}$  were randomly oriented.

Room temperature resistivity  $\rho$  (300 K) of the best layers approximates the values for epitaxial films prepared by pulsed laser deposition (PLD) or high density bulk materials [12–14].  $\rho(T)$  curves for  $\text{LaNiO}_3$ ,  $\text{CaRuO}_3$  and  $\text{La}_{0.5}\text{Sr}_{0.5}\text{CoO}_3$  thin films were metallic (Table II). Epitaxial layers possess lower resistivity than oriented polycrystalline ones.

TABLE II

Electrical resistivity of the films.

Film	Substrate	$\rho$ (300 K) [ $\text{m}\Omega \text{ cm}$ ]	$(1/\rho)(\Delta\rho/\Delta T)$ [ $1000/\text{K}$ ] (100–250 K)
$\text{CaRuO}_3$	YSZ	0.5	2.0
$\text{CaRuO}_3$	$\text{PrO}_x/\text{YSZ}$	0.38	1.4
$\text{La}_{0.5}\text{Sr}_{0.5}\text{CoO}_3$	$\text{LaAlO}_3$	0.35	2.6
$\text{La}_{0.5}\text{Sr}_{0.5}\text{CoO}_3$	MgO	0.85	2.0
$\text{LaNiO}_3$	MgO	0.46	2.2

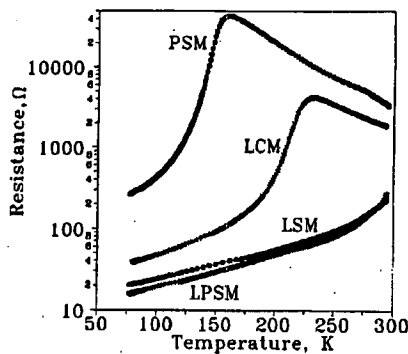


Fig. 2. The temperature dependence of resistivity of the films on  $\text{LaAlO}_3$ : PSM —  $\text{Pr}_{0.7}\text{Sr}_{0.3}\text{MnO}_3$ , LSM —  $\text{La}_{0.7}\text{Sr}_{0.3}\text{MnO}_3$ , LPSM —  $\text{La}_{0.35}\text{Pr}_{0.35}\text{Sr}_{0.3}\text{MnO}_3$ , LCM —  $\text{La}_{0.7}\text{Ca}_{0.3}\text{MnO}_3$ .

Temperature of M–I transition  $T_p$  in  $\text{R}_{1-x}\text{A}_x\text{MnO}_3$  can be presented in the form of a universal dependence on (R,A) radius (at a constant  $\text{Mn}^{4+}/\text{Mn}^{3+}$  ratio) [15, 16]. The maximum  $T_p$  value, which exceeds room temperature, answers  $\text{M} = \text{Sr}$  for  $x = 0.3$ . Our data (Fig. 2) is in agreement with the prediction.

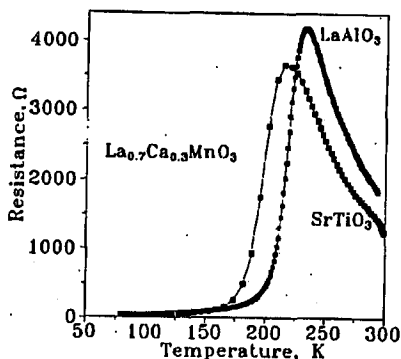


Fig. 3. The temperature dependence of resistivity of  $\text{La}_{0.7}\text{Ca}_{0.3}\text{MnO}_3$  films on  $\text{LaAlO}_3$  and  $\text{SrTiO}_3$ .

$\text{La}_{0.7}\text{Sr}_{0.3}\text{MnO}_3/\text{LaAlO}_3$  shows metal-like temperature dependence of the resistivity in the range 77–300 K with steeper resistivity increase approaching 300 K.  $\text{La}_{0.7}\text{Ca}_{0.3}\text{MnO}_3/\text{LaAlO}_3$  reveals maximum resistivity at 230 K. The value correlates with data for bulk and thin films of the same composition [15, 17]. Substitution of Pr for La initiates more complex behaviour.

$T_p$  of  $\text{La}_{1-x}\text{Ca}_x\text{MnO}_3$  films was known to be dependent on the substrate material [18]:  $\text{La}_{0.8}\text{Ca}_{0.2}\text{MnO}_3$  film on  $\text{MgO}$  had  $T_p = 240$  K and broader transition width than film on  $\text{LaAlO}_3$  ( $T_p = 270$  K). The origin of the behaviour was not elucidated in [18]: variation of lattice mismatch or variation of the epitaxial quality. To clarify the problem, we compared the  $\text{La}_{0.7}\text{Ca}_{0.3}\text{MnO}_3$  films on  $\text{LaAlO}_3$  and  $\text{SrTiO}_3$  being of practically the same epitaxial quality. Resistivity curves are very similar for both films (Fig. 3), but shifted  $\approx 20$  K. One can see that these substrates possess nearly equal but reverse lattice mismatch with the film. Since, in addition,  $T_p$  of the epitaxial films on  $\text{LaAlO}_3$  and  $\text{NdGaO}_3$ , the latter has very low lattice mismatch with the film ( $\approx 0.3\%$ ), are very close [18], we can conclude that tension but not constriction of the film in the plane of the interface results in the change of  $T_p$ .

This research was supported by VW Foundation grant I/69341 and RFBR grant 96-03-33027.

## References

- [1] R. Ramesh, H. Gilchrist, T. Sands, V.G. Keramidis, R. Haakeenasen, D.K. Fork, *Appl. Phys. Lett.* **63**, 3592 (1993).
- [2] K. Char, *MRS Bull.* **19**, 51 (1994).
- [3] T. Inoue, K. Eguchi, H. Arai, *Chem. Lett.*, 1939 (1988).
- [4] T. Arakawa, K. Takada, Y. Tsunemine, J. Shiokawa, *Sens. Actuators* **14**, 215 (1988).
- [5] D.B. Hibbert, R.H. Campbell, *Appl. Cat.* **41**, 289 (1988).
- [6] Y. Tokura, *Physica C* **235-240**, 138 (1994).
- [7] A.K. Raychaudhury, *Adv. Phys.* **44**, 21 (1995).
- [8] C.N.R. Rao, A.K. Cheetham, *Science* **272**, 369 (1996).

- [9] A.R. Kaul, B.V. Seleznev, *J. Phys. (France) IV Coll. C3* **3**, 375 (1993).
- [10] S.V. Samoylenkov, O.Yu. Gorbenko, I.E. Graboy, A.R. Kaul, Yu.D. Tretyakov, *J. Mater. Chem.* **6**, 623 (1996).
- [11] O.Yu. Gorbenko, V.N. Fuflyigin, Yu.Yu. Erokhin, I.E. Graboy, A.R. Kaul, Yu.D. Tretyakov, G. Wahl, L. Klippe, *J. Mater. Chem.* **4**, 1585 (1994).
- [12] S.G. Lee, K. Park, Y. Park, J. Park, *Appl. Phys. Lett.* **64**, 2028 (1994).
- [13] J.V. Mantese, A.L. Micheli, A.B. Catalan, N.W. Schubring, *Appl. Phys. Lett.* **64**, 3509 (1994).
- [14] H. Ichinose, Y. Shiwa, M. Nagano, *Jpn. J. Appl. Phys.* **33**, 5907 (1994).
- [15] H.Y. Hwang, S.W. Cheong, P.G. Radaelli, M. Marezio, B. Batlogg, *Phys. Rev. Lett.* **75**, 914 (1995).
- [16] P.G. Radaelli, M. Marezio, H.Y. Hwang, S.W. Cheong, *J. Solid State Chem.* **122**, 444 (1996).
- [17] G.J. Snyder, R. Hiskes, S. DiCarolis, M.R. Beasley, T.H. Geballe, *Phys. Rev. B* **53**, 14434 (1996).
- [18] Y.Q. Li, J. Zhang, S. Pombrik, S. DiMascio, W. Stevens, Y.F. Yan, N.P. Ong, *J. Mater. Res.* **10**, 2166 (1995).